

Prolonged vortex formation during the ejection period in the left ventricle with low ejection fraction: a study by vector flow mapping

Nobuaki Fukuda · Keiichi Itatani · Koichi Kimura · Aya Ebihara ·
Kazuaki Negishi · Kansei Uno · Kagami Miyaji · Masahiko Kurabayashi ·
Katsu Takenaka

Received: 25 November 2013 / Accepted: 15 January 2014 / Published online: 25 March 2014
© The Japan Society of Ultrasonics in Medicine 2014

Abstract

Purpose Vortex formation in the left ventricle (LV) can be visualized by novel vector flow mapping (VFM) based on color Doppler and speckle tracking data. The aim of this study was to evaluate the impact of a vortex during the ejection period using VFM.

Subjects and methods Color Doppler images were obtained to produce VFM images in 80 subjects (20 normal, 29 with dilated cardiomyopathy, and 31 with old myocardial infarction). The duration of the LV vortex was measured and expressed as the ratio to the ejection time (VTRe).

Results The VTRe showed significant correlations with EDV ($\rho = 0.672$, $p < 0.001$), ESV ($\rho = 0.772$, $p < 0.001$), EF ($\rho = -0.783$, $p < 0.001$), left atrium diameter (LAd) ($\rho = 0.302$, $p = 0.007$), stroke volume ($\rho = -0.600$, $p < 0.001$), e' ($\rho = -0.389$, $p < 0.001$), a' ($\rho = -0.314$, $p = 0.005$), s' ($\rho = -0.512$, $p < 0.001$), and E/e' ($\rho = 0.330$,

$p = 0.003$). The diastolic parameters (e' , a' , E/e' , LAd) were not correlated when they were adjusted by EF.

Conclusions In the normal LV, a vortex existed for only a limited time during the early ejection period. In contrast, the lower the EF was, the longer the vortex remained during systole. Evaluation of vortices by VFM may non-invasively provide novel insights into the pathophysiology of impaired cardiac function.

Keywords Vortex · VFM (vector flow mapping) · Color Doppler · Speckle tracking · Impaired cardiac function

Introduction

The heart is an organ that contracts and dilates regularly and continuously, pumping blood to the whole body. The blood stream and the pressure distribution are generated

N. Fukuda (✉) · M. Kurabayashi
Department of Medicine and Biological Science, Gunma
University Graduate School of Medicine, 3-39-22 Showa-machi,
Maebashi, Gunma 371-8511, Japan
e-mail: fukuda75@gmail.com

K. Itatani
Department of Hemodynamic Analysis, Kitasato University
School of Medicine, Sagamihara, Kanagawa, Japan

K. Kimura
Department of Cardiovascular Medicine, The University of
Tokyo Hospital, Tokyo, Japan

A. Ebihara
Department of Clinical Laboratory, The Cancer Institute
Hospital of JFCR, Tokyo, Japan

K. Negishi
Menzies Research Institute Tasmania, Hobart, TAS, Australia

K. Uno
Department of Computational Diagnostic Radiology and
Preventive Medicine, The University of Tokyo Hospital, Tokyo,
Japan

K. Miyaji
Department of Cardiovascular Surgery, Kitasato University
School of Medicine, Sagamihara, Kanagawa, Japan

K. Takenaka
Department of Cardiovascular Medicine, Nihon University of
Medicine, Itabashi Hospital, Tokyo, Japan

efficiently inside the heart chamber as it changes its shape. Cardiac dysfunction induces heart failure or left ventricular (LV) remodeling and changes the hemodynamics in the whole body [1, 2].

The blood flow in the LV has been investigated in studies using model experiments [3–5] and numerical simulations [6–9]. Several methods for visualizing blood flow in the LV are currently applied to human beings, such as cardiac magnetic resonance (CMR) [10–12] and contrast echocardiography including particle imaging velocimetry (PIV) [13–15]. These techniques have proven that vortices are formed in the LV around the mitral inflow. Vortices in the LV have been considered to be formed to achieve an efficient flow stream toward the outflow.

Color Doppler imaging can noninvasively visualize the blood flow velocities and is widely used for the clinical evaluation of cardiovascular diseases. Because Doppler methods are, by nature, dependent on the flow measurement angle, Ohtsuki and Tanaka proposed a flow vector visualization method named echo-dynamography (also known as vector flow mapping [VFM] [18]), based only on color Doppler data to overcome the limitation of Doppler measurements [16, 17]. However, their velocity vector estimation method had theoretical deficits, especially regarding the definition of the vortex flow and the near wall flow treatment. Recently, Garcia et al. [19] reported a new method based not only on the color Doppler data but also on the LV wall motion velocities obtained from wall tracking data. Their method is based on the continuity equation in the measurement plane, and is theoretically robust with regard to the setting of the boundary conditions using the wall tracking method, because B-mode two-dimensional speckle tracking images are based on the Cartesian coordinate and are not dependent on the beam angle. Further, Itatani et al. [20] have developed a new flow velocity vector visualization method based on a modification of Garcia's method by refining the weight function of the two numerical azimuthal velocity components derived from the bilateral ventricular wall boundaries, and this method has been validated by performing computational fluid dynamics (CFD) studies [20]. Their novel method is also called VFM, but the concept is completely different from the echo-dynamography or previous VFM reported by Tanaka, Ohtsuki, and Uejima [16–18]. This novel method may be a sensitive method for imaging the blood flow, especially in vortex flow structures and near wall flow. The aim of this study was to evaluate the role of the vortex flow during the ejection period using VFM.

Subjects and methods

The basic concept of the novel VFM

The basic concept of the novel version of VFM was first reported by Itatani, who modified Garcia's method, utilized both color Doppler information and LV wall speckle tracking information, and applied it to the human cardiovascular system [19, 20].

Blood flow visualization with VFM was based on the 2D continuity equation of the measurement plane expressed with a polar coordinate system (r, θ) centered at the sector probe (1). The apical long-axis view is used for the VFM analysis.

$$\partial_{\theta} V_{\theta} = -r \partial_r V_r - V_r \quad (1)$$

Because raw color Doppler data are too noisy to solve in a differential equation, sufficient data smoothing is necessary to stabilize the differential term. After median filtering within three neighboring points toward the radial direction (i.e., parallel to the ultrasound beam), color Doppler data are smoothed out with Gaussian filtering. The smoothed color Doppler data provide the radial velocity component (V_r). The azimuthal velocity component (V_{θ}) is given by the speckle tracking data of the ventricular wall after adjusting the non-slip boundary condition, in which ventricular wall motion directly affects the near wall blood flow, and in which the near wall flow velocity is equal to the ventricular wall velocity measured by the speckle tracking data.

Because the continuity Eq. (1) is the first-order differential equation, and speckle tracking data give two wall boundary conditions derived from the anteroseptal and posterior wall, two flow velocity fields are acquired ($V_{\theta+}$ and $V_{\theta-}$, respectively). V_{θ} was calculated by mixing the two fields according to a weight function (w), which denoted a normalized length from the anteroseptal wall boundary:

$$V_{\theta} = wV_{\theta-} + (1 - w)V_{\theta+}$$

The 2D velocity vector of the blood flow can then finally be depicted in the LV. (The algorithm is illustrated in Fig. 1.)

Data acquisition and analysis

All subjects were examined at rest in the left lateral decubitus position. The echocardiographic examinations were performed with commercially available equipment

Fig. 1 A flowchart of the VFM algorithm

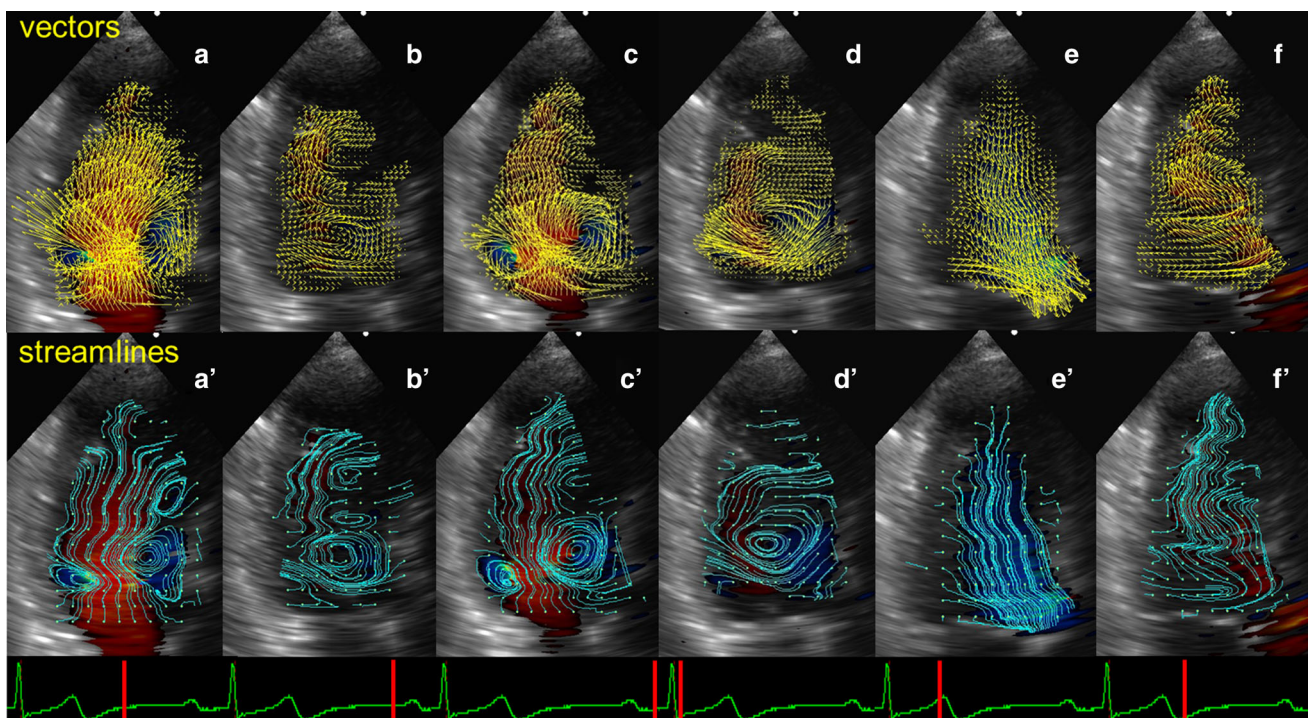
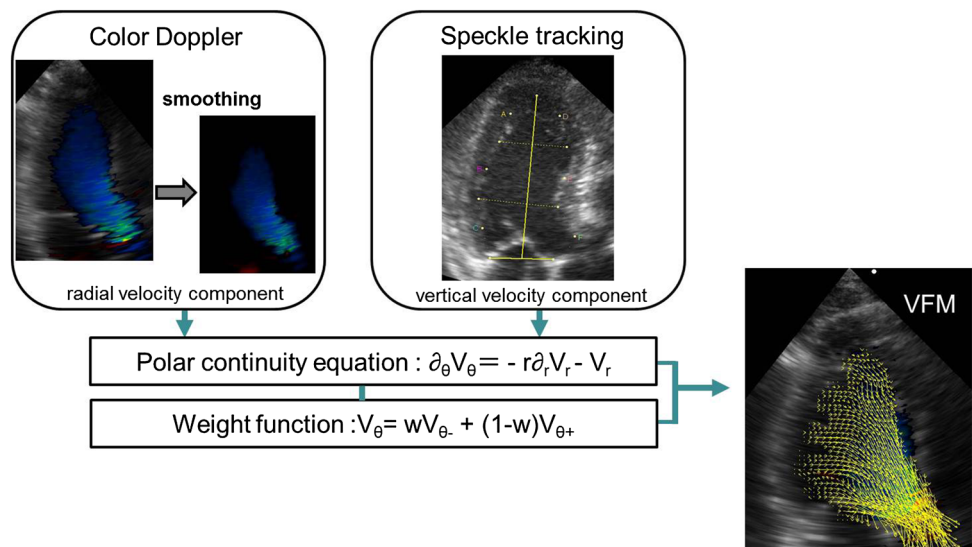


Fig. 2 The LV blood flow vectors and streamlines in one cardiac cycle. The upper row displays the flow vectors and the lower row shows the streamlines. In early diastole (a, a'), two vortices were formed around the bilateral side of the transmitral inflow, and the one beneath the anterior mitral leaflet was larger in size than the other formed beneath the posterior mitral leaflet. During the mid- (b, b') to late-diastolic phase, the dominant anterior side vortex was gradually attenuated. During the atrial contraction period (c, c'), vortices were

formed again around the transmitral flow. The vortex remained until the isovolumic contraction time (d, d'). During the ejection period (e, e'), a laminar outflow was directed toward the aortic valve, and the vortex decreased in size and finally disappeared during the early phase of systole. During the mid-systolic phase, straight streamlines were observed. During the isovolumetric relaxation time (IRT) (f, f'), the LV flow was reversed, and was thus directed toward the apex

(Prosound α10; Hitachi-Aloka Medical, Tokyo, Japan). Images were obtained using a 1.0- to 5.0-MHz broadband ultrasound transducer. The LV end-diastolic volume (EDV), end-systolic volume (ESV), and ejection fraction

(EF) were assessed by biplane Simpson's rule using the apical 4- and 2-chamber views. A normal EF is defined as 55 % or higher in this study. The stroke volume (SV) was assessed by pulsed wave Doppler over the LV outflow tract

[21]. The mitral inflow was recorded, and the peak Doppler velocities of early filling (E wave) and atrial kick (A wave) were measured. Tissue Doppler velocities (early diastolic annular velocity, e' ; late diastolic annular velocity, a' ; systolic annular velocity, s') were then acquired at the septal and lateral mitral annular sites, and they were averaged [22]. The left atrial diameter (LAd) from M-mode, guided by the parasternal long-axis image at the level of the aortic valve, was measured.

Color Doppler data for VFM were acquired in the apical long-axis view, which included the LV apex, mitral inflow, and LV outflow tract, and which could measure the dominant blood flow generated in the LV. The mean temporal resolution was 22 ± 3.2 ms (45 ± 5.3 frames/s) in this study. At least three consecutive beats were stored, and the data were analyzed off-line using a software program for VFM (Hitachi-Aloka Medical, Tokyo, Japan). The velocity vector fields were indicated with yellow arrows (Fig. 2), in which a 1-cm arrow length was compatible to a 40-cm/s flow velocity in the present study. In addition, to clarify the shape of the vortex, streamlines were drawn (Fig. 2).

Quantitative evaluation of the vortex during the ejection period

Based on the physiology of the blood flow in the LV, we quantitatively evaluated the vortex flow, especially during the early ejection period, because it is closely related to the LV outflow and is considered to be directly related to the efficiency of the ejection by the ventricular wall motion. In the present study, a vortex was defined as a collection of streamlines which made a curved flow and returned to a starting point after having moved some distance from the starting point. The criteria of the vortex formation were described as follows: D is the farthest distance from a starting point in a streamline and P is the distance between the starting point and the closest point in the streamline to the starting point after it reached the farthest distance (Fig. 3). We defined R as follows:

$$R = \frac{P}{D}$$

We defined a streamline as a vortex which satisfies $R < 0.4$. The ejection time was defined as the time from the onset to termination of LV ejection as determined by pulsed wave Doppler of the LV outflow tract. The frame numbers of the LV vortex existence during the ejection time (VT: vortex time) were measured from VFM images, and the vortex time ratio to the ejection time (VTRe) was expressed as the ratio to all frame numbers during the ejection time (ET).

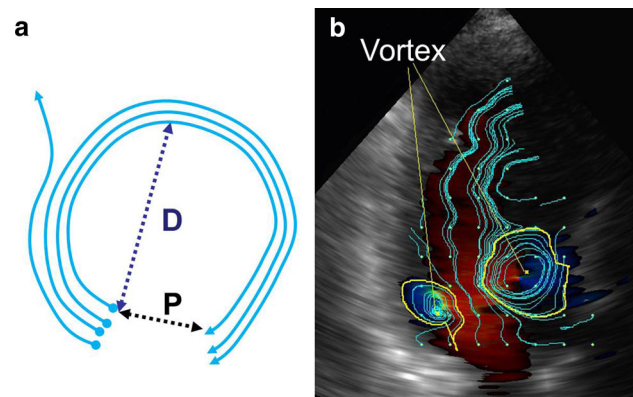


Fig. 3 Definition of a vortex. **a** D is the farthest distance from the starting point in a streamline, and P is the distance between the starting point and the closest point in the streamline to the starting point after it reached the farthest distance. R is calculated as P/D . A vortex is defined as a streamline which satisfies $R < 0.4$. **b** Vortices are automatically detected. Two yellow loops indicate vortices which satisfied the definition of a streamline

$$\text{VTRe} = \frac{\text{VT}}{\text{ET}}$$

The VTRe was calculated as the average value of three consecutive heart beats.

Study population

Eighty subjects who underwent an echocardiographic examination in the laboratory of the University of Tokyo Hospital were investigated in the present study. Their mean age was 59 ± 17 years, and the male:female ratio was 60:20. Of all 80, 20 were healthy subjects without previous cardiac disease, 29 were diagnosed with dilated cardiomyopathy (DCM), and 31 were diagnosed with old myocardial infarction (OMI). All DCM and OMI patients had low ejection fractions. The sites of the OMI were antero-septal in 13 patients, inferior in six, inferior and posterior in five, and inferior and anterior in seven patients.

Patients with chronic atrial fibrillation, significant aortic and mitral valve disease, post-aortic or mitral valve replacement, congenital heart disease, hypertrophic cardiomyopathy, an unstable hemodynamic state, such as acute myocardial infarction or congestive heart failure, and images of insufficient quality were excluded from this study.

The study protocol was approved by the institutional Ethics Committee of the University of Tokyo Hospital, and all patients gave written informed consent for their participation.

Statistical analysis

The continuous data were presented as the mean ± standard deviation, and categorical data were expressed as percentages unless otherwise specified. Normality was evaluated by the Kolmogorov–Smirnov test. Because the VTRe was not normally distributed, Spearman’s rho was used to express correlation. Comparisons between groups were presented as the median ± quartile deviation and were assessed using the Mann–Whitney *U* test. In order to evaluate the confounding relationships, diastolic parameters were entered into the multiple linear regression models using rank-transformed VTRe as a dependent variable and the EF as another covariate. The statistical analyses were performed with the SPSS version 16.0 software program (SPSS Inc., Chicago, IL, USA), and two-sided values of *p* < 0.05 were considered to be statistically significant.

Results

The LV blood flow vectors and streamlines in one cardiac cycle

The normal LV vortex formation process observed in the VFM is illustrated in Fig. 2. The subject was a male with a normal LV function and normal hemodynamics, with an EF = 62 %, E wave velocity = 71 cm/s, and A wave velocity = 50 cm/s. In early diastole, two vortices were formed around the bilateral side of the transmitral inflow, and the one beneath the anterior mitral leaflet was larger in size than the other formed beneath the posterior mitral leaflet. During the mid- to late-diastolic phase, the dominant anterior side vortex gradually attenuated. During the atrial contraction period, vortices formed again around the transmitral flow. During the isovolumetric contraction time (ICT), a vortex was preserved in the basal to mid portion of the LV. In the ejection period, a laminar outflow was directed toward the aortic valve, and the vortex decreased in size and finally disappeared during the early phase of the systole. During the mid-systolic phase, straight streamlines were observed. In the isovolumetric relaxation time (IRT), the LV flow was reversed, and was directed toward the apex.

Echocardiographic data

The echocardiographic variables of the subjects in this study are shown in Table 1. The twenty healthy subjects had a normal EF, and all 60 subjects with OMI or DCM had a reduced EF.

The subjects in the normal EF group were younger than those with a reduced EF. There were no significant

Table 1 Baseline echocardiographic characteristics in the normal and reduced EF groups

	Normal EF	Reduced EF	<i>p</i> value
<i>n</i>	20	60	
Male/female	15/5	45/15	NS
Age (y.o.)	48 ± 19	62 ± 15	0.009
Underlying disease	None	OMI 31/DCM 29	
HR (/min)	65 ± 10	73 ± 19	NS
EDV (ml)	82 ± 19	151 ± 61	<0.001
ESV (ml)	28 ± 9	101 ± 53	<0.001
EF (%)	66 ± 5	36 ± 11	<0.001
SV (ml)	76 ± 13	56 ± 17	<0.001
E wave velocity (cm/s)	67 ± 16	67 ± 31	NS
A wave velocity (cm/s)	59 ± 22	65 ± 21	NS
<i>e'</i> velocity (cm/s)	10.3 ± 4.0	5.6 ± 2.3	<0.001
<i>a'</i> velocity (cm/s)	8.8 ± 3.3	7.5 ± 2.7	NS
<i>s</i> velocity (cm/s)	8.4 ± 1.7	5.5 ± 1.9	<0.001
E/ <i>e'</i>	7.1 ± 2.3	13.3 ± 7.9	0.001
LAd (mm)	35 ± 5	44 ± 8	<0.001

A normal EF was defined as 55 % or higher. A reduced EF was defined as lower than 55 %

HR heart rate, EDV end-diastolic volume, ESV end-systolic volume, EF ejection fraction, SV stroke volume, LAd left atrial diameter, OMI old myocardial infarction, DCM dilated cardiomyopathy

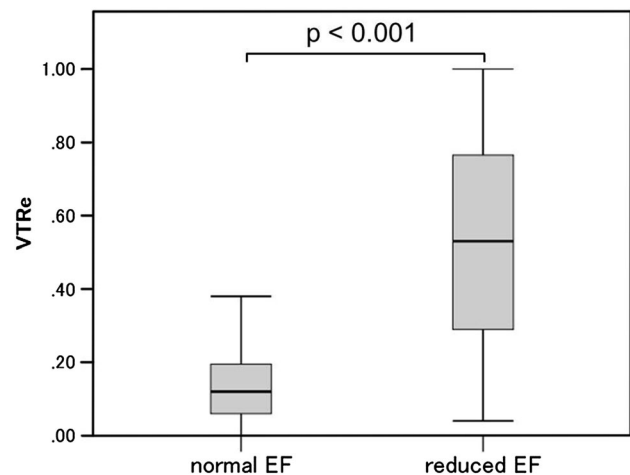


Fig. 4 The VTRe was compared between the normal EF group and reduced EF group. The median VTRe (0.12 and 0.53, normal EF group and reduced EF group, respectively) is indicated by horizontal bars. The vertical bars indicate the range, and the horizontal boundaries of the boxes represent the first and third quartiles

differences in the gender between the groups. The EDV, ESV, and LAd were significantly larger, the EF, SV, *e'* velocity, and *s'* velocity were lower, and the E/*e'* was higher in the reduced EF group. The heart rate, E wave velocity, A wave velocity, and *a'* velocity were not significantly different between the groups.

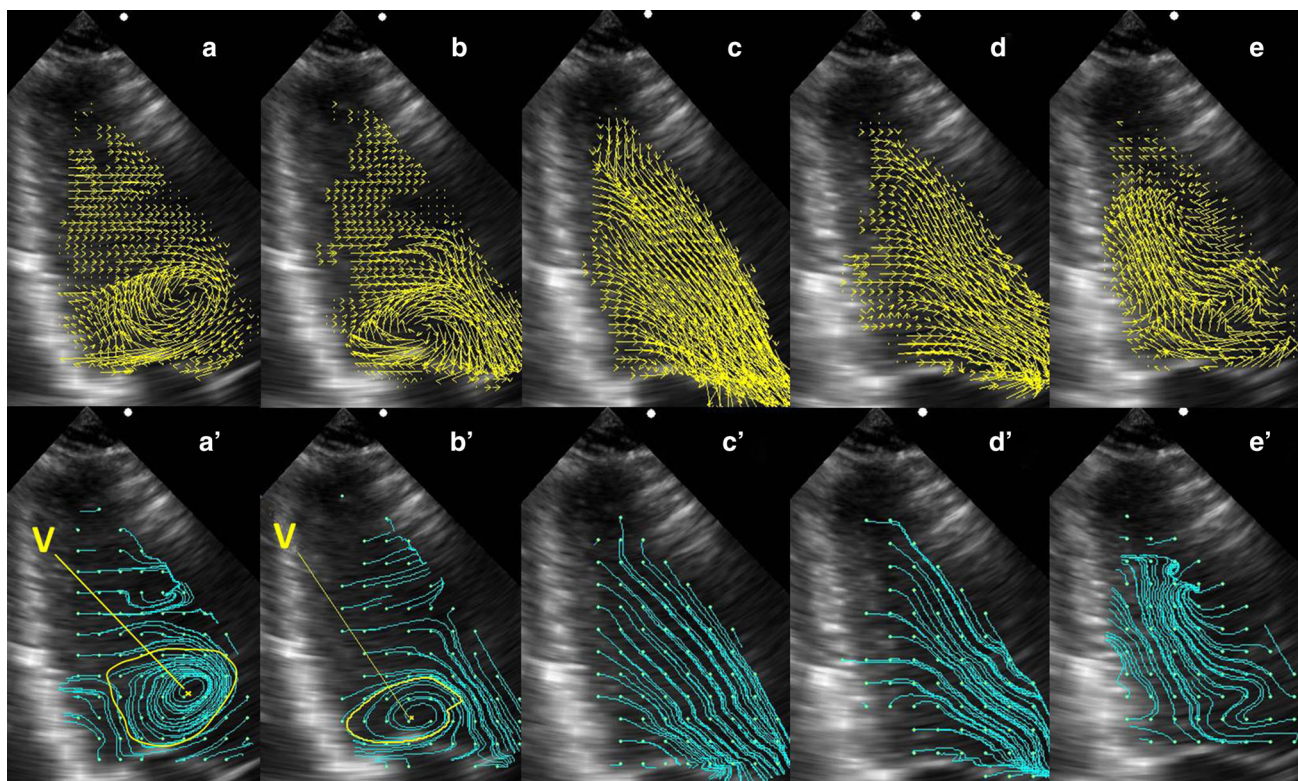


Fig. 5 The VFM in the ejection period in a healthy subject. **a, a'** ICT, **b, b'** the early ejection phase, **c, c'** the middle ejection phase, **d, d'** the late ejection phase, and **e, e'** IRT. The subject had a normal volume and EF (EDV = 91 ml, ESV = 35 ml, EF = 62 %). There was a

vortex (V) in the LV in ICT. Although the vortex persisted at the early phase, only flows which went toward the aorta were observed from the middle to late phases during the ejection period. The VTRe was 0.14 in this case

VTRe

The VTRe in the subjects with a reduced EF was significantly higher than that in healthy subjects (0.53 ± 0.24 vs 0.12 ± 0.07 , $p < 0.001$) (Fig. 4).

Typical intraventricular flow vectors of a healthy subject during ejection period are illustrated in Fig. 5. This subject had a normal volume and EF (EDV = 91 ml, ESV = 35 ml, EF = 62 %). In ICT, a vortex was formed in the basal to mid portion of the LV. At the beginning of the ejection period, the vortex remained at the basal portion just behind the straightforward outflow. The vortex disappeared soon after that, and then the straight laminar flow was sustained until the aortic valve closed. In this case, the VTRe was calculated to be 0.14 for the average of three heart beats. In all subjects with a normal EF, the vortex similarly disappeared in the early period of the ejection phase, and the VTRe was < 0.4 .

The flow vector fields in a subject with DCM are shown in Fig. 6. The subject had a large LV volume and reduced EF (EDV = 177 ml, ESV = 122 ml, EF = 31 %). Compared with the healthy subjects, the vortex in the ICT was larger. Complex flows added some vortices during the ejection period. Vortices also persisted in IRT. They were

also preserved throughout the ICT, ejection period, and IRT. In this case, the VTRe was calculated to be 1.00 for the average of three heart beats. In the reduced EF group, vortices appeared for a longer time than in the normal EF group. There were three patients (5 % of the reduced EF group) with vortices that persisted during the whole LV ejection phase in this study.

The scatter diagrams in Fig. 7 show the relationships between the VTRe and other conventional systolic and diastolic parameters. The VTRe showed a significant positive, but modest, correlation with the EDV ($\rho = 0.672$, $p < 0.001$) and ESV ($\rho = 0.772$, $p < 0.001$), as well as weak positive correlations with the E/e' ($\rho = 0.330$, $p = 0.003$) and LAAd ($\rho = 0.302$, $p = 0.007$). The negative correlation with the EF ($\rho = -0.783$, $p < 0.001$) was the strongest, followed by a negative correlation with the SV ($\rho = -0.600$, $p < 0.001$), s' ($\rho = -0.512$, $p < 0.001$), e' ($\rho = -0.389$, $p < 0.001$), and a' ($\rho = -0.314$, $p = 0.005$). However, there were no correlations between the VTR and the E and A wave velocities ($r = 0.056$, $p = \text{NS}$; $r = -0.078$, $p = \text{NS}$, respectively). The VTRe had a higher value when the systolic function and diastolic function were reduced and the LV volume was large. But in the multivariate linear regression analyses, diastolic

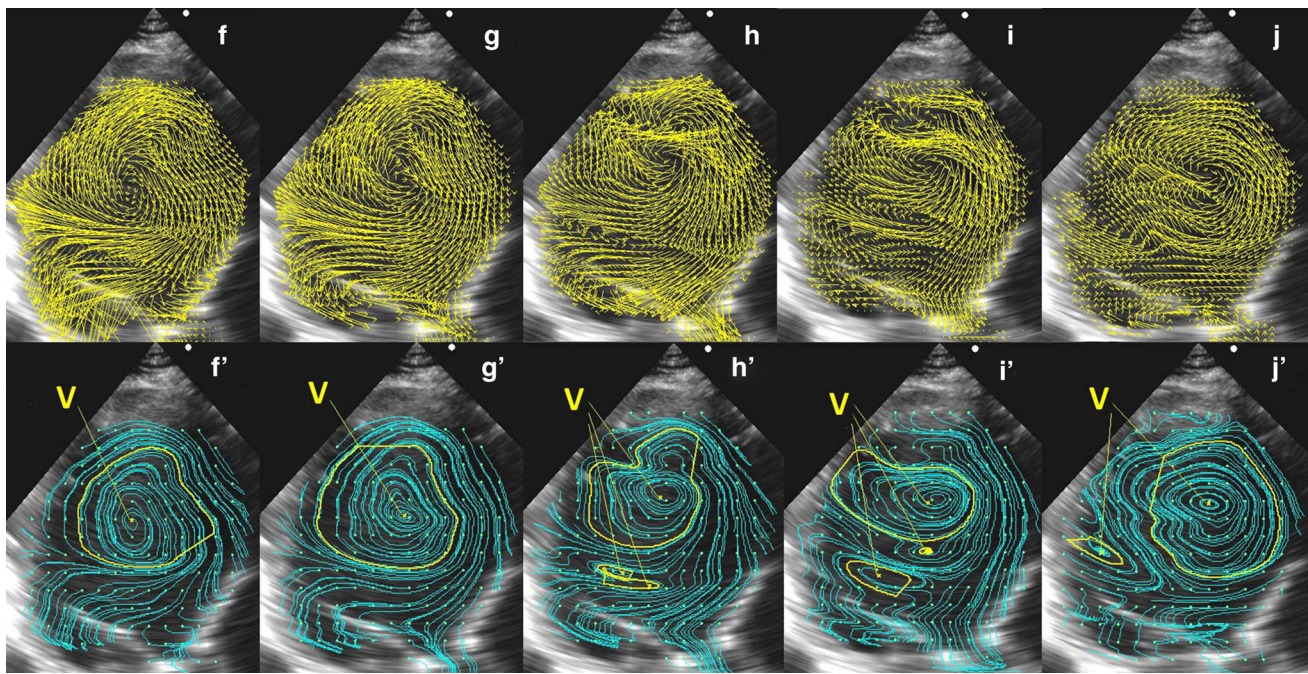


Fig. 6 The VFM in the ejection period in a subject with DCM. **f, f'** ICT, **g, g'** the early ejection phase, **h, h'** the middle ejection phase, **i, i'** the late ejection phase, and **j, j'** IRT. The subject had a large LV volume and a reduced EF (EDV = 177 ml, ESV = 122 ml,

EF = 31 %). A large vortex (V) occupied the LV in ICT. The vortices were observed throughout the ejection period. The VTRe was 1.00 in this case

parameters (e' , a' , E/e' , LAd) that were relatively weakly correlated with the VTRe in the univariate linear regression analysis were not correlated when they were adjusted by the EF.

The VTRe and EF in the subgroup of reduced EF are summarized in Table 2. There was a significant difference among them (VTRe, $p = 0.032$; EF, $p = 0.003$). After adjusting with EF, there was no significant difference in VTRe among the subgroup ($p = 0.24$).

Discussion

The present study investigated the vortices in the human LV during the ejection period, and the influences of impaired LV function on the vortex formation and degeneration process inside the chamber were revealed by using VFM based on color Doppler and speckle tracking data.

Recently, some studies have visualized and quantified the blood flow in the human LV. Their visualization methods have included numerical simulations [6–9], CMR [10, 11], and contrast echocardiography including PIV [13–15]. According to the findings obtained from their results, the mitral inflow immediately forms a pair of counter-rotating vortices which are asymmetrical in size, and the one behind the anterior mitral leaflet is dominant. These vortices are considered to be generated from the inlet jet

shear layer that rolls up due to the viscous forces exerted onto the jet core [6, 8]. In the IVC, the anterior vortex is preserved in the LV. Straight outflow streamlines are observed when the cardiac muscle contracts during the ejection phase. The vortex under the mitral valve disappears as the LV chamber volume decreases. In the IRT period, the blood flow redirects to the apex, and the process is caused by the LV sucking force during diastole [24]. Similar phenomena were observed also by VFM (Fig. 2). It is considered that vortices not only efficiently change the direction of the flow but also avoid flow collision, resulting in minimized energy expenditure [11, 15]. The asymmetries and curvatures of the looped heart in humans are believed to enable more efficient hemodynamics [11]. The vortices formed in the LV reflect cardiac function and morphology; thus, abnormalities in the vortex formation process may reflect the presence of underlying suboptimal hemodynamics in the dysfunctional LV.

Most of the previous reports have analyzed and discussed the vortices formed during diastole, and the significance of vortices during systole has not been revealed [13–15]. In the present study, we revealed that the VTRe significantly increased in patients with OMI and DCM, and that systolic function correlated with the VTRe. On the other hand, the VTRe is not independently related to the filling velocity (E and A wave velocity) or diastolic function indices (e' , a' , E/e' , LAd). In normal subjects, as the basal posterior wall

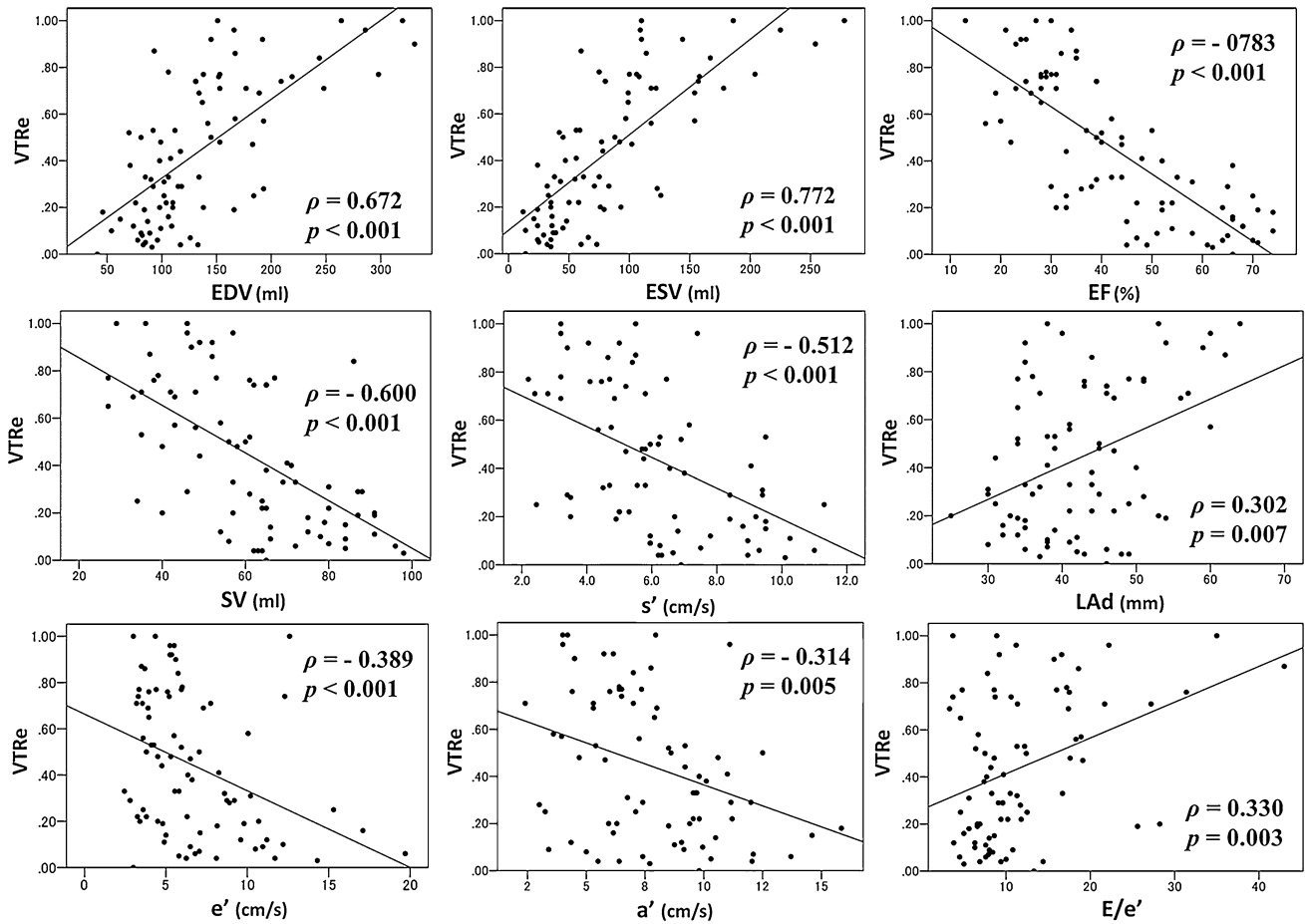


Fig. 7 The correlation between the VTRe and conventional echo parameters. The VTRe was significantly positively correlated with the EDV, ESV, E/e' , and LAd, negatively correlated with the EF, SV, e' ,

a' , and s , and not correlated with the E and A waves. ρ , a correlation coefficient; p , p value

Table 2 VTRe and EF in the subgroup of reduced EF

	<i>N</i>	VTRe	EF (%)
Anteroseptal OMI	13	0.45 ± 0.24	36 ± 6
ant. and inf. OMI	7	0.59 ± 0.33	29 ± 9
inf. OMI	6	0.41 ± 0.21	45 ± 10
inf. and post. OMI	5	0.29 ± 0.21	49 ± 5
DCM	29	0.64 ± 0.28	33 ± 10

ant. anterior, inf. inferior, post. posterior, OMI old myocardial infarction, DCM dilated cardiomyopathy, EF ejection fraction

contracted, the space beneath the mitral valve decreased and became so small that the vortex could not remain, but was absorbed with the outflow stream. On the other hand, in subjects with a reduced EF, the ESV increased and the cardiac output decreased, resulting in an enlarged postero-basal space sufficient to form a vortex even in the mid- or late-systolic phase. Sometimes, the persisting vortex during the ejection period was divided into two or more vortices, but the size, number, and location drastically changed at

each moment. The flow was inefficient and energy was dissipated, resulting in the excessive consumption of oxygen in these subjects [6]. Hong et al. [15] reported in his study using PIV that a vortex was sustained during the whole cardiac cycle from the diastolic period to the whole systolic period in patients with abnormal LV systolic function, and their results are consistent with our present results. Presumably, vortices that persist until the late-systolic phase or even until the IRT period would disturb the apically directed inflow, resulting in a weakened LV sucking force or diastolic function. Therefore, we speculate that a persistent LV vortex to the late-systolic phase is not only associated with the energetic inefficiencies of the systolic contraction work performed by the LV wall motion but also associated with the reduced transmission of the power force created by the active sucking accompanied by the LV wall relaxation.

The present study is the first reported clinical research study in which the novel VFM was applied in cases with normal and diseased ventricular functions. Evaluation of the vortex formation process may be useful to reveal the

pathophysiology of the disadvantageous blood flow caused by impaired cardiac function, or to reveal the mechanisms of LV remodeling in patients with heart failure. Remodeling is a compensatory change, and is the process by which the ventricular size, shape, and function are regulated by the hemodynamic load and neurohormonal and genetic factors [1, 2]. To compensate for a reduced EF and stroke volume, the LV volume is generally enlarged. In our study, the EF was strongly correlated with the ESV ($r = -0.905$, $p < 0.001$). Diastolic dysfunction develops early in most cardiac diseases, and echographic diastolic function indices also provide prognostic information about heart failure due to OMI or DCM [22]. The EF was correlated with the diastolic function indices e' ($r = 0.545$, $p < 0.001$), a' ($r = 0.498$, $p < 0.001$), E/e' ($r = -0.468$, $p < 0.001$), and LAd ($r = -0.404$, $p < 0.001$) in our study. The VTRe was correlated with not only the systolic function and LV volume but also with some diastolic function indices (e' , a' , E/e' , and LAd) in the univariate regression analysis, but it was not correlated with the diastolic function indices in a multivariate regression analysis. This means that the VTRe is only an index of the systolic phase. Further examinations are warranted to specifically clarify how the reduced cardiac function or the dilated ventricular volume individually affects the vortex formation pattern. Zhang et al. [25] investigated the vortices during the ejection period using the previous VFM. They reported that the LV end-systolic short diameter, but not the EF, was an independent predictor of the duration of vortex persistence. Although some results similar to those in the present study were obtained, the definition and the method used to measure the vortex flow are completely different. In the previous VFM concept, the color Doppler data were divided into a vortical flow component and a nonvortical basic flow component [17, 18]. Then, a stream function of the vortical flow component and a novel flow function were applied to the basic flow component, and were used to solve the azimuthal velocity value in the measurement plane. The problem is the existence and uniqueness of the flow division method with regard to the vortical and basal flow. Moreover, the definition of a vortex is unclear in this oversimplified assumption. The novel VFM concept is based on the 2D mass flow conservation assumption, and flow vectors and streamlines are depicted based on color Doppler data and wall motion velocity data, and vortices are automatically extracted from the images by a clear mathematical definition.

The temporal resolution (22 ± 3.2 ms) in this study was between PIV (16.4 ± 3.5 ms) [15] and CMR (25–50 ms) [8–10, 12, 26]. The flow velocity in VFM can be analyzed up to two times during the aliasing velocity (130 cm/s in the present study). On CMR the temporal resolution is relatively low, the scan time is long, and it is also more

expensive than echocardiography. PIV excels in the temporal resolution. The analytical flow velocity is limited (60 cm/s or less) because of particle migration out of the scan plane [15], and it is not sufficient for flow velocity analysis in the human heart. VFM would therefore be a useful modality to assess the hemodynamics and function of the ventricle.

Study limitations

In the present study, we measured only the duration of the presence of vortices during systole, but did not quantify the vortex itself. It would be ideal for ejection blood to flow in one direction towards the aorta, but in patients with low EF, the efficiency of LV function seems to be impaired since the vortex flow persisted without being ejected into the aorta. However, in order to evaluate such functional efficiency accurately, it is necessary to not only evaluate the pattern of the vector field but also directly quantify the energy efficiency. The influences of these vortex characteristics on the patients' ventricular function warrant further study.

Itatani et al. [20] validated the accuracy of VFM with CFD studies and proved that their method achieved accurate flow visualization, especially in terms of near wall flow measurement and vortex flow detection. They verified their method using simple flow models and in vivo blood flow in the ventricular chamber of a normal subject, but did not note the complicated blood flow in the diseased heart chamber. In addition, a gold standard method has not yet been established for the quantitative evaluation of vortices in vivo. In the present study, we established a definition of "vortex" based on the shape of the streamlines to avoid ambiguity of the vortical flow often observed in the complicated turbulent flow in the dilated heart chamber.

In the present study, even the subjects with impaired systolic function had stable hemodynamics, and we did not evaluate the acute phase of the systolic dysfunction. Moreover, in the present study, there were no patients with pure diastolic dysfunction. Further studies are required to analyze a wider range of ventricular disorders.

Conclusions

We have shown the characteristic of the vortex in the LV during the ejection period using VFM. In the normal LV, the vortex was found for only a limited time during the early ejection period. In contrast, the lower the EF is, the longer the vortex remains during systole. Evaluation of vortices with VFM may noninvasively provide novel insights into the pathophysiology of impaired cardiac function.

Conflict of interest The authors declare no conflict of interest associated with this manuscript.

Ethical considerations All procedures followed were in accordance with the ethical standards of the responsible committee on human experimentation (institutional and national) and with the Helsinki Declaration of 1975, as revised in 2008 (5). Informed consent was obtained from all patients for being included in the study.

References

- Cohn JN, Ferrari R, Sharpe N. Cardiac remodeling—concepts and clinical implications: a consensus paper from an international forum on cardiac remodeling. Behalf of an international forum on cardiac remodeling. *J Am Coll Cardiol.* 2000;35:569–82.
- Sutton MG, Sharpe N. Left ventricular remodeling after myocardial infarction: pathophysiology and therapy. *Circulation.* 2000;101:2981–8.
- Bellhouse BJ, Bellhouse FH. Fluid mechanics of the mitral valve. *Nature.* 1969;224:615–6.
- Bellhouse BJ. Fluid mechanics of a model mitral valve. *J Physiol.* 1970;207:72P–3P.
- Kheradvar A, Gharib M. On mitral valve dynamics and its connection to early diastolic flow. *Ann Biomed Eng.* 2009;37:1–13.
- Pedrizzetti G, Domenichini F. Nature optimizes the swirling flow in the human left ventricle. *Phys Rev Lett.* 2005;95:108101.
- Nakamura M, Wada S, Yamaguchi T. Influence of the opening mode of the mitral valve orifice on intraventricular hemodynamics. *Ann Biomed Eng.* 2006;34:927–35.
- Schenkel T, Malve M, Reik M, et al. MRI-based CFD analysis of flow in a human left ventricle: methodology and application to a healthy heart. *Ann Biomed Eng.* 2009;37:503–15.
- Saber NR, Wood NB, Gosman AD, et al. Progress towards patient-specific computational flow modeling of the left heart via combination of magnetic resonance imaging with computational fluid dynamics. *Ann Biomed Eng.* 2003;31:42–52.
- Kim WY, Walker PG, Pedersen EM, et al. Left ventricular blood flow patterns in normal subjects: a quantitative analysis by three-dimensional magnetic resonance velocity mapping. *J Am Coll Cardiol.* 1995;26:224–38.
- Kilner PJ, Yang GZ, Wilkes AJ, et al. Asymmetric redirection of flow through the heart. *Nature.* 2000;404:759–61.
- Markl M, Kilner PJ, Ebbers T. Comprehensive 4D velocity mapping of the heart and great vessels by cardiovascular magnetic resonance. *J Cardiovasc Magn Reson.* 2011;13:7.
- Sengupta PP, Khandheria BK, Korinek J, et al. Left ventricular isovolumic flow sequence during sinus and paced rhythms: new insights from use of high-resolution Doppler and ultrasonic digital particle imaging velocimetry. *J Am Coll Cardiol.* 2007;49:899–908.
- Ishizu T, Seo Y, Ishimitsu T, et al. The wake of a large vortex is associated with intraventricular filling delay in impaired left ventricles with a pseudonormalized transmitral flow pattern. *Echocardiography.* 2006;23:369–75.
- Hong GR, Pedrizzetti G, Tonti G, et al. Characterization and quantification of vortex flow in the human left ventricle by contrast echocardiography using vector particle image velocimetry. *JACC Cardiovasc Imaging.* 2008;1:705–17.
- Tanaka M, Sakamoto T, Sugawara S, et al. Blood flow structure and dynamics, and ejection mechanism in the left ventricle: analysis using echo-dynamography. *J Cardiol.* 2008;52:86–101.
- Ohtsuki S, Tanaka M. The flow velocity distribution from the Doppler information on a plane in three-dimensional flow. *J Vis.* 2006;9:69–82.
- Uejima T, Koike A, Sawada H, et al. A new echocardiographic method for identifying vortex flow in the left ventricle: numerical validation. *Ultrasound Med Biol.* 2010;36:772–88.
- Garcia DDAJ, Tanne D, Yotti R, et al. Two-dimensional intraventricular flow mapping by digital processing conventional color-Doppler echocardiography images. *IEEE Trans Med Imaging.* 2010;29:1701–13.
- Itatani K, Uejima T, Tanaka T, et al. Intraventricular flow velocity vector visualization based on the continuity equation and measurements of vorticity and wall shear stress. *Jpn J Appl Phys.* 2013;52:07HF16.
- Quinones MA, Otto CM, Stoddard M, et al. Recommendations for quantification of Doppler echocardiography: a report from the Doppler quantification Task force of the nomenclature and standards committee of the American Society of Echocardiography. *J Am Soc Echocardiogr.* 2002;15:167–84.
- Nagueh SF, Appleton CP, Gillebert TC, et al. Recommendations for the evaluation of left ventricular diastolic function by echocardiography. *J Am Soc Echocardiogr.* 2009;22:107–33.
- Iwase HLH, Fujimoto S, Himeno R. Computational modeling of left ventricle dynamics and flow based on ultrasonographic data. *JSME Int J Ser C.* 2003;46:1321–9.
- Ohte N, Narita H, Akita S, et al. The mechanism of emergence and clinical significance of apically directed intraventricular flow during isovolumic relaxation. *J Am Soc Echocardiogr.* 2002;15:715–22.
- Zhang H, Liu L, Chen L, et al. The evolution of intraventricular vortex during ejection studied by using vector flow mapping. *Echocardiography.* 2013;30:27–36.
- Sengupta PP, Pedrizzetti G, Kilner PJ, et al. Emerging trends in CV flow visualization. *JACC Cardiovasc Imaging.* 2012;5:305–16.